Environ Monit Assess (2016) 188:697
DOI 10.1007/s10661-016-5656-x

Use of ultra-high spatial resolution aerial imagery in the estimation of chaparral wildfire fuel loads

Ian T. Schmidt · John F. O'Leary · Douglas A. Stow · Kellie A. Uyeda · Phillip J. Riggan

Received: 3 April 2016 / Accepted: 20 October 2016

Abstract Development of methods that more accurately estimate spatial distributions of fuel loads in shrublands allows for improved understanding of ecological processes such as wildfire behavior and postburn recovery. The goal of this study is to develop and test remote sensing methods to upscale field estimates of shrubland fuel to broader-scale biomass estimates using ultra-high spatial resolution imagery captured by a light-sport aircraft. The study is conducted on chaparral shrublands located in eastern San Diego County, CA, USA. We measured the fuel load in the field using a regression relationship between basal area and aboveground biomass of shrubs and estimated ground areal coverage of individual shrub species by using ultra-high spatial resolution imagery and image processing routines. Study results show a strong relationship between image-derived shrub coverage and field-measured fuel loads in three even-age stands that have regrown approximately 7, 28, and 68 years since last wildfire. We conducted ordinary least square analysis using ground coverage as the independent variable regressed against biomass. The analysis yielded R^2 values ranging from 0.80 to 0.96 in the older stands for the live shrub species, while R^2 values for species in the younger stands ranged from 0.32 to 0.89. Pooling species-based data into larger sample sizes consisting of a functional group and all-shrub classes while obtaining suitable linear regression models supports the potential for these methods to be used for upscaling fuel estimates to broader areal extents, without having to classify and map shrubland vegetation at the species level.

Keywords Southern California · Chaparral · Wildfire · Biomass · Fuel load estimation · Ultra-high-resolution imagery

Introduction

The classic "fire environmental triangle" comprised three components: topography, weather conditions, and fuel properties (Countryman 1972). Topography and weather conditions are readily measured, while fuel properties are difficult to estimate due to high variability over time and space. Fuel properties are generally organized into four categories when modeling wildfire behavior: (1) fuel type, (2) fuel loading, (3) fuel condition, and (4) fuel moisture (Dennison et al. 2006). Quantification of plant biomass is recognized as an integral component in the study of numerous ecological processes including fire spread and intensity as well as recovery from wildfires (Riggan et al. 1988; Catchpole and Wheeler 1992, Riggan et al. 1994). Accurate estimates of the amount and spatial distribution of wildfire fuel are critical when modeling and predicting fire behavior.

I. T. Schmidt (✉) · J. F. O'Leary · D. A. Stow · K. A. Uyeda
Department of Geography, San Diego State University, San Diego, CA 92182-4493, USA
e-mail: ian.schmidt@sdcounty.ca.gov

P. J. Riggan
Pacific Southwest Research Station, 4955 Canyon Crest Drive, Riverside, CA 92507, USA

Published online: 28 November 2016

Development of methods that improve aboveground biomass (AGB) estimates will improve fire spread modeling by contributing a more comprehensive data set that takes into account fuel heterogeneity. Decision support systems for fire suppression and fuel management currently in place rely on fuel models that assume fuel load homogeneity, thus limiting their effectiveness in predicting fire behavior (Arroyo et al. 2008).

Field-based AGB estimation is more accurate for individual plants and small patches but is usually limited in areal coverage and spatial distribution due to accessibility and extensive field personnel requirements. Field-based measurement of biomass is extremely labor intensive and even estimates based on sampling and statistical relationships are particularly challenging in dense shrublands which can be almost impenetrable and commonly occur on very steep slopes. Conversely, a remote sensing (RS) approach enables much greater areal coverage than field-based methods, but validating RS-based areal estimates of biomass is challenging and rife with uncertainty (Lu 2006; Chen et al. 2009; Garcia et al. 2010; Eisfelder et al. 2011). In general, RS is the preferred method to estimate AGB over relatively large areas (Lu 2006; Nijland et al. 2009). Regression approaches used to estimate AGB are common due to their ability to more tractably estimate AGB with a high degree of efficiency and certainty (Catchpole and Wheeler 1992).

Several low-cost remote sensing systems employing high (or ultra-high) spatial resolution imagery have been developed recently. Satellite-based systems also collect high-resolution imagery, but not as detailed as an unmanned aircraft system or light-sport aircraft platform-based systems due to the close distance between the sensor and the ground for the aircraft platforms (Lu 2006). Ultra-high-resolution imagery has been recognized as a potential data source for upscaling field-based fuel load estimates to larger areal coverage imagery (Eisfelder et al. 2011).

Chaparral, the semi-arid shrubland-type examined in this study, is of particular interest for fuel load research due to the role it plays in the complex wildfire regime of Southern California. Chaparral is a highly flammable wildfire fuel that covers most of the Mediterranean-climate rangeland in Southern California and is often located in close proximity to large human populations. Chaparral is dominated by evergreen sclerophyllous shrubs that are typically deep rooted and is located on the foothills of San Diego County, primarily on steep slopes between 150 and 1600 m elevation. Wildfires are a common feature of the chaparral environment, and the community as a whole is resilient to wildfire (Horton and Kraebel 1955; Hanes 1971; Keeley 1991; Conard and Weise 1998). Urban sprawl within large areas of chaparral has created a recipe for catastrophic wildfire events (e.g., the 2003 Cedar Fire in San Diego County).

The overall goal of this study is to develop and test methods for the estimation of stand-level fuel loading (or biomass per unit area) in chaparral shrublands using RS technology coupled with field-based measurements of AGB. Ultra-high spatial resolution true color imagery collected from a light-sport aircraft is explored in the context of estimating the areal ground coverage of shrub species within permanent sample plots. The level of spatial resolution in this study needs to be as detailed as possible due to the necessity of accurate species identification and ground coverage measurements. Evaluating the ability to obtain relatively accurate fuel load estimates by means of image-based species identification has the potential to contribute to upscaling approaches where ground-based fuel estimates may be extrapolated to larger areal extents. Mapping and estimating ground coverage of shrubs through processing and analysis of aerial imagery are considerably more efficient than using ground-based methods, underscoring the rationale to evaluate the potential of the methods developed in this study for upscaling to stands or ground resolution elements of satellite imagery.

Specifically, in this study, we use imagery with ultra-high spatial resolution coupled with field-derived fuel load estimates as the primary data sets to accomplish the following tasks: (1) derive ground-based fuel load estimates within sample plots using a regression analysis approach, (2) estimate ground coverage of the dominant shrub species within sample plots using remote sensing, and (3) generate statistical models and cross-validate model results to address the co-variance between ground coverage and biomass estimates.

Materials and methods

Study area

The study area comprised two sites, each located south of Mt. Laguna in the Cleveland National Forest, approximately 65 km east of San Diego, CA, USA (Fig. 1a). The first site is located near Kitchen Creek and the second is about 5 km east of the Kitchen Creek site in Long Canyon. Sample plots at both study sites are located on steep east-facing slopes at elevations of approximately 1420–1530 m. The soils are classified as fine loamy, mixed, mesic, and mollic haploxeralf, derived from quartz diorite and mica schist (Bowman 1973). The region has a Mediterranean-type climate with 93 % of annual precipitation occurring October–April. The average annual precipitation is 66 cm (PRISM Climate Group 2014; http://prism.oregonstate.edu), and the mean annual temperature is 12.9 °C (Riggan et al. 1988).

The vegetation of the study area is composed of mixed chaparral dominated by the shrub species *Quercus berberidifolia* and *Adenostoma fasciculatum* with lesser amounts of *Arctostaphylos glandulosa*, *Ceanothus perplexans*, and *Salvia apiana* admixed. The study area contains vegetation stands of three age classes (7, approximately 28, and 68 years at the time of the original field and image data acquisition). The youngest (7 years old) stand is located within the Long Canyon site where prescribed burning was conducted in 2005. The next youngest (approximately 28 years old) stand is located at the Kitchen Creek site where a series of strip-shaped experimental fires (parallel to slope) were conducted between the years of 1979–1985. The remaining vegetation at the Kitchen Creek site is the oldest as it burned in 1944 during a large wildfire event. Locations of the experimental fires were clearly defined from visual interpretation of multi-spectral aerial imagery collected shortly after the experimental burns (1985), provided by the USDA Forest Service. Burned areas interpreted from the imagery were digitized using GIS methods and loaded onto a handheld GPS to allow for identification in the field.

Field methods

Fifteen permanent sample plots were established throughout the study area as part of a combined sampling effort with another related study (Uyeda et al. 2016). Each plot measured 64 m^2 (8 m × 8 m). Five plots were located in each of the three age classes for a total of 15 sample plots (Fig. 1). Shrub cover in the Kitchen Creek area is extremely dense, and access to these plots was facilitated by a trail cut through the study area by a fire crew from the US Forest Service. All plots in the Kitchen Creek area are located within 50 m of the trail. Another consideration for plot selection was that at least one plot exhibited low, medium, and high normalized difference vegetation index values in each stand age (derived from historical imagery). The corners of each plot are marked with rebar stakes and digitally recorded as coordinates gathered with a Trimble GeoXM handheld global positioning system (GPS) unit with a postprocessed accuracy of 1 to 3 m. Procedures for deriving AGB per unit area estimates are outlined in Table 1 and elaborated below. We measured all-shrub stems 0.4 cm or more in diameter within each plot at 10 cm above the ground using digital calipers and recorded the species of the stem and whether it was live, dead, or charred. We recorded the minimum and maximum stem diameters of irregularly shaped stems to determine average stem diameters. We identified live stems by the presence of green leaves, so stems that appeared mostly dead were counted as live if green leaves were present.

We harvested live, dead, and, for the 7-year-old area, charred stems from the most abundant species (*A. fasciculatum*, *Q. berberidifolia*, *A. glandulosa*, *C. perplexans*) near the sampling plots to determine field weight and basal diameter. We typically sampled one species per day and selected one shrub per day to serve as a representative sample to estimate the ratio of dry-to-wet weights. Each representative shrub was taken to the lab where we separated it into small (<0.5 cm), medium (0.5 to 2.0 cm), and large (>2.0 cm) diameter fractions. We weighed each size fraction and subsampled it to determine water content. We dried the samples to a constant weight in a drying oven at 100 °C. We determined the total shrub water content by applying the appropriate water content value to the biomass of each shrub fraction to calculate average water content scaled by size fraction. This value was then applied to all shrubs sampled on that day. This sampling occurred mostly in autumn and early winter seasons from 2011 to 2013.

We calculated the coefficients for the relationship of dry aboveground biomass (AGB) as a power function of stem basal area (BA) with a bias correction applied (Baskerville 1972; Sprugel 1983):

$$\mathrm{AGB} = B_0(\mathrm{BA})^{B_1} e^{0.5\ s}$$

where s is the residual mean square, B_0 is the proportionality coefficient, and B_1 is the scaling exponent.

In order to optimize time spent in the field, we generated species and age-specific equations for each

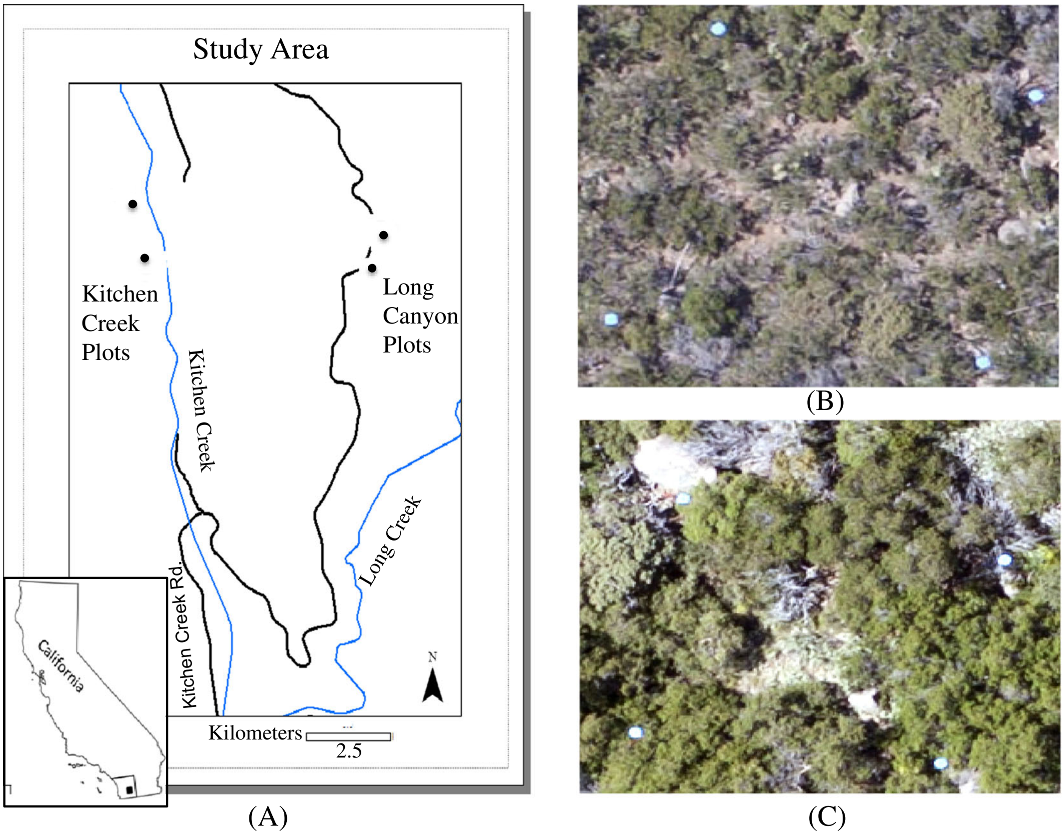

Fig. 1 **a** Study area map depicting the sampling plot locations at both study sites. **b** Ultra-high spatial resolution imagery of sampling plot 2 (within the 68-year-old stand). **c** Ultra-high spatial resolution imagery of sampling plot 3 (within the 7-year-old stand)

species in the burned areas where they were most abundant. For example, *Q. berberidifolia* occurred infrequently in the 7-year-old area, so we used the equation from the 28-year-old area rather than generating a new equation. We also produced a generic equation for each age class using the pooled measurements across all species to provide an estimate for less-abundant species. We calculated aboveground biomass for entirely dead shrubs that could not be identified by species using the generic dead shrub equation for the appropriate burn year. We only occasionally found charred stems in the older stands, so we estimated charred biomass in these areas by using half the value given by the appropriate equation for dead biomass.

Image data

In order to efficiently characterize the fuel properties of each age class, we classified imagery from the 68- and 28-year-old age classes of chaparral using color (RGB) aerial imagery collected in June 2012 using a 21-megapixel camera. A light-sport aircraft flew approximately 150 m above ground level, allowing for the capture of ultra-high spatial resolution imagery (5 to 7 cm ground sampling distance) using a digital single-lens reflex camera. The medium format digital camera allowed for the capture of a high spatial resolution color image for each sampling plot. The imagery served as the primary data source in the estimation of areal ground coverage of shrub species found in the sample plots.

Digital orthoimagery commissioned and made available from the National Geospatial Intelligence Agency was used as reference data for geoprocessing of the aerial imagery. The orthoimagery has a ground sampling distance of 30 cm, and the source imagery was captured by a Leica ADS-40 airborne digital line array sensor.

Image preprocessing

We completed four processing steps to prepare imagery for the classification: (1) extraction of raw data, (2) subsetting or clipping of scenes containing sampling

Table 1 Summary of upscaling procedures

Steps
1. Cut and weigh approximately 10 representative shrubs per species
2. Establish the basal area (BA) to above ground biomass (AGB) regression relationship by species
3. Per plot:
i. Measure BA and record species
ii. Calculate AGB by applying species-specific regression relationships for each stem measurement
iii. Capture and georeference/rectify NEOS image
iv. Digitize polygons delineating all individual and coalescing shrub canopies by species
v. Edit polygons at the sampling plot
vi. Determine areal cover using the calculate geometry function in ArcMap for each polygon
vii. Sum of areal cover by species
viii. Calculate AGB/area by dividing total AGB by total shrub area
4. Regress AGB on ground cover estimates (m^2) per species for all plots
i. Group species with similar functional groups and repeat regressions
ii. Calculate predicted AGB with the LOOCV statistical method

plots from entire image, (3) geometric correction of image subsets, and (4) corner locations of the sampling plots on geocorrected image subsets. The RGB imagery was geometrically corrected using the ground control point (GCP) correction tool within the ERDAS Imagine software. This enabled image-to-map rectification and geographic referencing (i.e., georeferencing) of the raw imagery from the aerial imaging flight using the true color orthoimagery as reference data. We applied the correction to generate imagery with planimetric geometry, thus removing most systematic errors (Jensen 2005) and allowing for more accurate estimates of ground vegetation coverage. Geometric correction and georeferencing were necessary for achieving uniform scale across image frames when measuring the distance or area of ground elements, e.g., shrub ground coverage, as scale variations existed in the raw imagery for most of the scenes that contained irregular topography.

We geometrically corrected the subset images covering each of the plots for the Kitchen Creek site separately; images of the plots at the Long Canyon site were corrected in a single transformation. Approximately 25–35 GCPs per image subset were selected by visually identifying ground features (typically boulders) in both the raw ultra-high-resolution images and orthoimagery. RMSE values for the polynomial warping function used for the geometric transformation ranged from 0.03 to 0.31 pixels.

Three of the 15 sampling plots contained plot corner markers identifiable when viewing the ultra-high spatial resolution imagery. We tied blue plastic plates, each 26 cm in diameter, to the top of the canopy above the four corners of each sample plot. We oriented the plates parallel to and above the canopy to maximize their exposure. We used blue-colored plates because they provided the highest contrast to the green canopy of chaparral and ensured the precise location of each sampling plot on the imagery. Determining accurate plot locations on the imagery is critical for this type of study because the ground areal coverage of each functional group is estimated for the sample plots. Errors in sample plot locations could result in unreliable estimates of areal extent of composition in areas of high heterogeneous species composition and biomass distributions.

Shrub species mapping and ground coverage estimates

We mapped shrub cover for the four most common species (*Q. berberidifolia*, *C. perplexans*, *A. fasciculatum*, and *A. glandulosa*). We also mapped all other shrub species as a single category (including less abundant shrubs and subshrubs such as *Cercocarpus betuloides*, *Rhamnus ilicifolia*, *Eriogonum fasciculatum*, *S. apiana*, and *Keckiella ternata*).

In addition, we created four aggregated categories (functional group 1, functional group 2, completely dead shrubs, and all-shrubs). Functional group 1 includes *Q. berberidifolia* and *C. perplexans*, which have broader leaves and are more spectrally differentiable than the shrubs of functional group 2, which includes *A. fasciculutum*, *A. glandulosa*, and all remaining shrubs and subshrubs. We included completely dead shrubs of any species in the scheme due to their frequent occurrence in sample plots at the Kitchen Creek site and the capability of the ultra-high-resolution imagery to potentially differentiate them. The final category, all-shrubs, is an aggregation of all shrubs and subshrub species found in the plots.

Individual shrub crowns within the patches are generally closed (i.e., each shrub crown projects 100 % cover of foliage and stems), making the delineation of individuals virtually impossible within shrub patches from an image analysis standpoint. In fact, discerning individual shrubs on the ground can be difficult, mainly due to underground basal burls that can cause uncertainty of connections belowground and branch inter-digitization. The patches frequently contain dozens of individuals that cover several square meters.

We primarily conducted the shrub species mapping process using on-screen visual image interpretation and “heads up” digitization of individual plant or vegetation patch polygons. ESRI ArcMap 10.1 and ERDAS Imagine were the primary software tools used in the classification process. We based the general stepwise approach on five steps to estimating species-based ground area coverage in the sampling plots: (1) creation of preliminary polygons around shrubs using heads-up digitization; (2) classification of polygons based on visual interpretation of color, texture, and density; (3) inspection of polygon delineations on the ground for 13 of the 15 sampling plots; (4) editing of preliminary polygons and classification assignments using results from step 3; and (5) calculation of the ground coverage area of the polygons using ArcGIS.

The field-based inspection increased the accuracy of the ground area estimates and added only a small amount of additional labor in the field. The inspection process included handwritten edits on diagrams in the field that contained the polygons overlaid on the ultra-high-resolution imagery. We were able to directly compare the accuracy and specificity of the preliminary polygons at each sampling plot. Several species-specific characteristics are discernible with the ultra-high spatial resolution imagery. For example, *Q. berberidifolia* foliage is considerably darker in color and denser than *A. fasciculatum* foliage, while *A. glandulosa* foliage is a light green color and is equally dense as *Q. berberidifolia* foliage.

We analyzed data for the Long Canyon and Kitchen Creek study areas independently due to the large discrepancy in time since last wildfire (7 vs. 28+ years). We pooled data for the 10 sampling plots at the Kitchen Creek study area because no measurable difference in AGB per plot was observed between the stands that burned in 1944 and 1985. We calculated stand AGB (kg m^{-2}) for each plot by dividing its total AGB by total shrub cover.

Statistical analysis

We regressed the AGB values against the ground coverage estimates for the most abundantly occurring species, creating linear models that could be used to predict fuel loads by measuring ground coverage alone. We compared the coefficient of determination (R^2) aggregated classes (completely dead, functional group 1, functional group 2, all-shrub stems).

We calculated the predicted AGB with the leave-one-out cross-validation (K-fold ($n - 1$)) statistical method (Kohavi, 1995). A point representing a perfect prediction falls onto the zero value axis (y), while points above zero are undervalued and negative points are overvalued.

Results

Field-based estimates of fuel loads

Table 2 displays the AGB estimates derived using the regression approach. The AGB estimate values within the Kitchen Creek plots (Uyeda et al. 2016) are generally much higher than those in the Long Canyon study site, e.g., the total AGB estimate for sampling plots at Kitchen Creek are all above 3.4 kg m^{-2}, while none of the sampling plots at Long Canyon were greater than 1.62 kg m^{-2}. Clearly, *Q. berberidifolia and A. fasciculatum* are the dominant species at the Kitchen Creek site, while *A. fasciculatum* and *C. perplexans* occurred most frequently at the Long Canyon sampling plots.

Shrub maps and coverage estimates

Figure 2 portrays the species type maps (overlaid on the original color aerial images) used to estimate ground area coverage by shrub species. The Long Canyon study area has considerably more bare ground than the Kitchen Creek, very likely due to the relatively short time since the last burn. The three sampling plots in Long Canyon were the only established sampling plots at the time of the flight campaign. A large individual *Q. berberidifolia* shrub was omitted in sampling plot 15 (top center) due to not being rooted in the sampling plot. Table 3 contains species ground coverage estimates derived from the shrub species maps presented in Fig. 2.

Linear regression and cross-validation

Figure 3 contains the sample points and the linear regression models for the species-based functional groups at the Kitchen Creek study area. There were a total of 10 sampling plots at the Kitchen Creek study area though

Table 2 Above ground biomass estimates (kg m^{-2})

Sampling plot	1	2	3	4	10	5	6	7	8	11	9	12	13	14	15
Quercus berberidifolia	5.68	1.16	3.26	0.34	5.04	0.57	3.09	0.35	0.40	1.91	0	0	0	0.10	0.14
Adenostoma fasciculatum	0.10	1.98	0	3.09	0	1.64	0.04	2.08	2.09	0.48	0.86	0.91	0.91	0.84	0.37
Ceanothus perplexans	0	0	0	0	0	1.08	0.11	0.53	0.49	1.55	0.18	0.50	0.31	0.10	0.41
Arctostaphylos glandulosa	0	0.49	0	0	0.20	0.07	0.35	0.02	0.49	0	0	0.00	0.11	0.42	0
All other shrubs	0.24	0.09	0.25	0	0.91	0.05	0.19	0.27	0.51	0.57	0.14	0.02	0.02	0.16	0.13
Completely dead	0.13	0.16	0.68	0.05	1.31	0	1.26	0.22	0	0	0.05	0	0	0	0.01
Plot sum	6.14	3.88	4.19	3.60	7.49	3.41	5.19	3.57	4.04	4.50	1.16	1.43	1.35	1.62	1.06

Plots are organized by burn history; Kitchen Creek sampling plots 1–4 and 10 last burned in 1944, Kitchen Creek plots 5–8 and 11 last burned in 1979–1985, and Long Canyon plots 12–15 and 9 last burned in 2005

not every plot contained all of the species. Therefore, the sample size (n) for regressions was less than 10 in most cases, except with *Q. berberidifolia* that occurred in every sampling plot. Five of the six models are generally comparable in slope and R^2 values. However, the entirely dead class had lower R^2 values than the other five classes.

The variability between the plots at Long Canyon (Fig. 4) is slightly higher than those for the Kitchen Creek plots due to the discrepancy in stand age and lower sample size. *C. perplexans* at the Long Canyon study area had an R^2 of 0.79 although the remaining species-based functional groups had either low values or could not be determined due to small sample size ($n \geq 2$). Species-based models at the Long Canyon study area are not suitable to estimate AGB alone, thus requiring the pooling of the samples into group types and all-shrub groups.

Two functional groups were created by pooling species-level data based on the similarity of slopes of ordinary least square (OLS) models: (1) *Q. berberidifolia* and *C. perplexans* and (2) the remaining shrub classes. At the Long Canyon site, the same groups were used as the Kitchen Creek site for continuity. Combining *Q. berberidifolia* and *C. perplexans* yielded moderate R^2 values at the Long Canyon site, while the *C. perplexans* alone yielded much greater R^2 values. Regression models were generated using a combination of all of the live species at both study areas. Due to the occurrence of completely dead stems at the Kitchen Creek site, an additional model was generated that combined live and dead materials. The models with both the data pooled into functional groups and all shrubs were included to support the potential of the methods to be applied for upscaling AGB estimates to stands with same burn history or ground resolution element associated with satellite imagery.

Table 4 contains the R^2 values derived from the cross-validation. The substantial amount of labor required to the sample plots restricted the sample size in some classes. The cross-validation for the Kitchen Creek plots indicates a high level of stability across *Q. berberidifolia* and *A. fasciculatum*, a moderate amount for *A. glandulosa*, and lesser amounts for the remaining classes. Figures 5 and 6 contain scatterplots containing the field-based estimates of AGB on the x-axis and field-based minus the K-fold predicted values on the y-axis. The general purposes of Figs. 5 and 6 are to display the distribution of the predicted values relative to that observed using K-fold ($n - 1$) and to assess for over/under prediction trends. Bivariate normal density ellipses were added to display any trends in the scatterplots that are not discernable looking at points alone. The ellipses show a slight upward trend at both study areas, meaning that sampling plots with greater AGB were underestimated slightly and sampling plots with lower AGB were slightly overestimated. The small upward trend is likely not large enough to affect results substantially.

Discussion and conclusions

When AGB was regressed on area of coverage, we found substantial variations in the R^2 values among species, functional groups, and all-shrub species groups in both study areas. Species-level classes at the Kitchen Creek site showed considerably higher R^2 values for the two most frequently occurring classes, *Q. berberidifolia* and *A. fasciculatum*, with values of 0.90 and 0.96, respectively. The R^2 values for *A. glandulosa*, *C. perplexans*, and the "all other shrub species" classes ranged from 0.80 to 0.87, showing a relatively strong

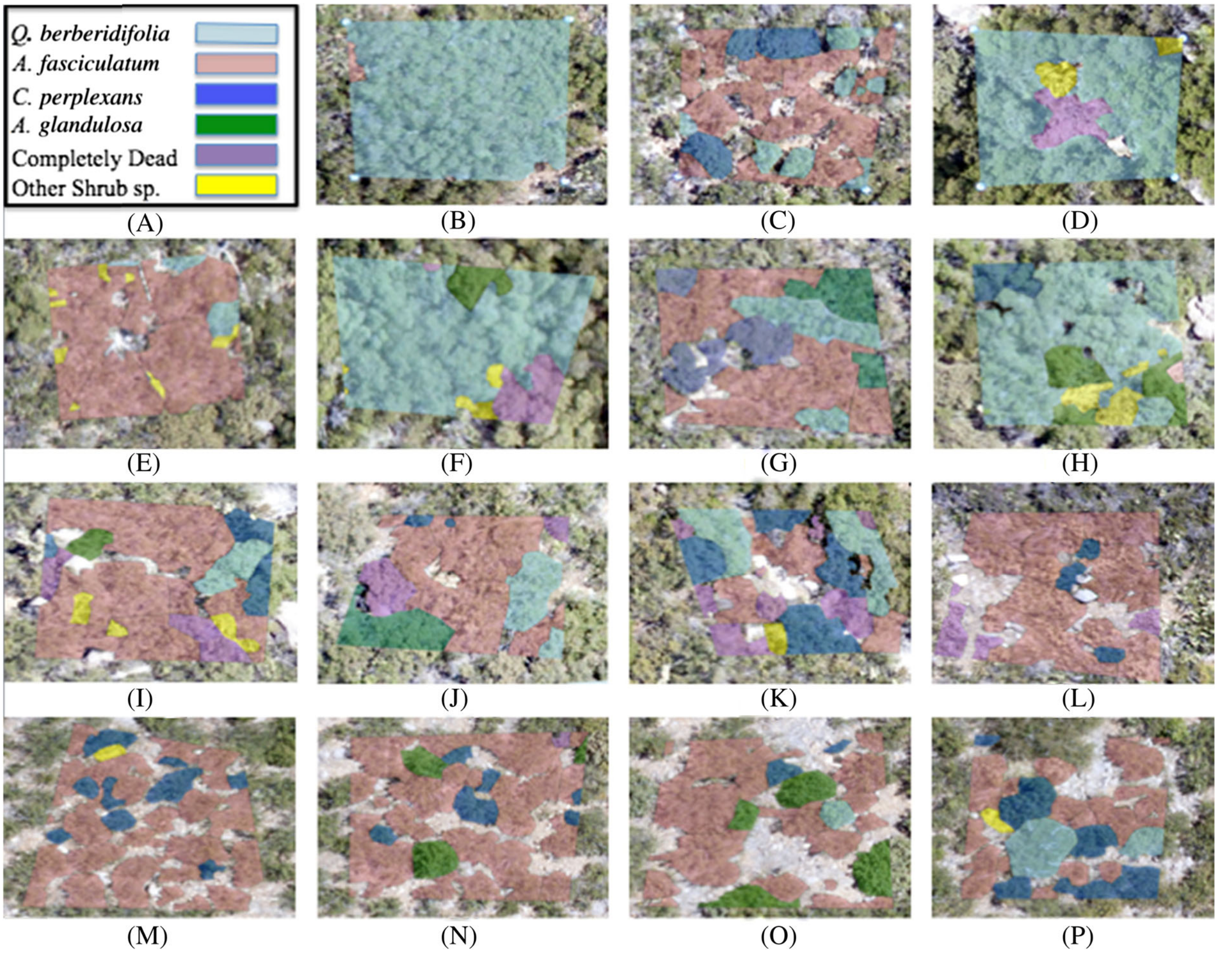

Fig. 2 Shrub species maps: **a** legend, **b** sampling plot 1, **c** sampling plot 2, **d** sampling plot 3, **e** sampling plot 4, **f** sampling plot 10, **g** sampling plot 5, **h** sampling plot 6, **i** sampling plot 7, **j** sampling plot 8, **k** sampling plot 11, **l** sampling plot 9, **m** sampling plot 12, **n** sampling plot 13, **o** sampling plot 14, and **p** sampling plot 15. Sampling plots 1–4 and 10 are located in the Kitchen Creek study area last burned in 1944; sampling plots 5–8 and 11 are located in the Kitchen Creek study area burned in early 1980s; and sampling plots 9 and 12–15 are located in the Long Canyon study area last burned in 2005. *Plastic plates* demarcating the sample plot corners are visible in Fig. 2b–d

Table 3 Ground coverage estimates in m^2 for shrub classification categories

Sampling plot	1	2	3	4	10	5	6	7	8	11	9	12	13	14	15
Quercus berberidifolia	61	7	48	3	43	3	42	4	8	11	0	0	0	1	8
Adenostoma fasciculatum	1	30	0	52	0	35	1	38	31	11	39	32	38	22	27
Ceanothus perplexans	0	0	0	0	0	10	4	4	5	14	2	7	3	1	13
Arctostaphylos glandulosa	0	8	0	0	3	3	9	0.4	7	0	0	0	4	6	0
All other shrubs	DNI	DNI	5	0	10	DNI	DNI	5	5	10	4	0.5	0.3	DNI	1
Completely dead	DNI	DNI	3	3	2	0	4	2	0	0	DNI	0	0	0	DNI

DNI indicates that a class was estimated at a sampling plot and not identified in the imagery. Zero values indicate that the sampling plot did not contain that shrub species/class

DNI did not identify

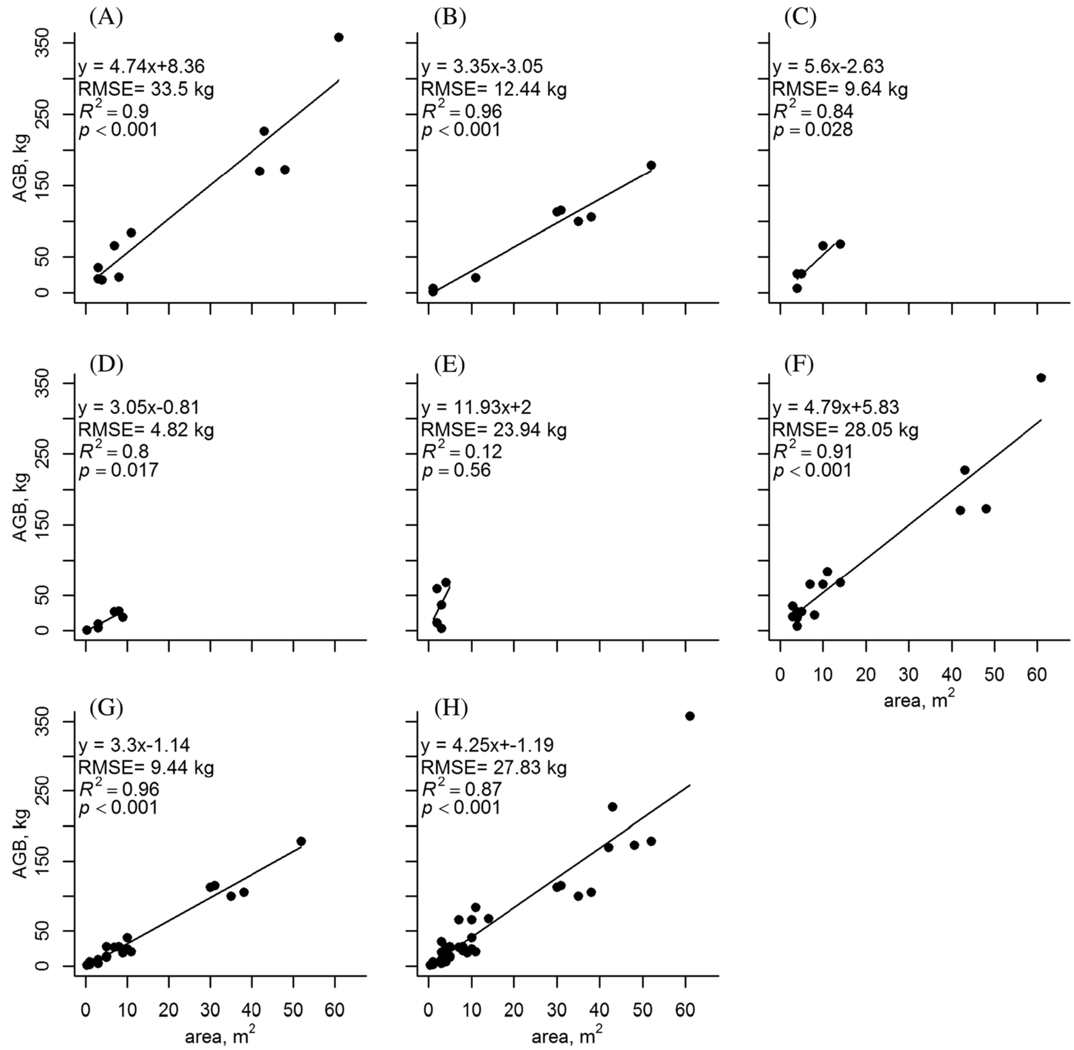

Fig. 3 Ordinary least square linear regression models at the Kitchen Creek study site. **a** *Quercus berberidifolia*, **b** *Adenostoma fasciculatum*, **c** *Ceanothus perplexans*, **d** *Arctostaphylos glandulosa*, **e** completely dead, **f** group 1, **g** group 2, and **h** all-shrubs

predictive relationship. The completely dead class at the Kitchen Creek site did not exhibit a significant relationship between area coverage and biomass with an R^2 value of 0.12 and a sample size of 5. The weak relationship is likely due to the difficulty of identifying completely dead stems intermixed with live stems based on visual interpretation of ultra-high spatial resolution RGB imagery. By contrast, the dead stems are readily identifiable in the field. Groups 1 and 2 had relatively high R^2 values (0.96 and 0.91, respectively) when OLS was applied at the Kitchen Creek site. The all-shrub pooled group had an R^2 value of 0.87. This indicates that if highly accurate fuel loads are required, then functional groups should be used to estimate fuel loads and that it is likely not necessary to sample shrubs at the species level.

The R^2 values for the younger-age chaparral at the Long Canyon site at the species-level were more variable than those of the Kitchen Creek site, and half of the species-level classes had invalid linear models. The three species-based models were invalid due to two reasons: (1) completely dead stems did not occur at the Long Canyon site, and (2) the small sampling size was inadequate to create an OLS model. *Q. berberidifolia* and *A. glandulosa* were only present in two sampling plots. The R^2 values for *A. fasciculatum* were much lower in the Long Canyon vs. the Kitchen Creek site, i.e., 0.32 vs. 0.90. Unlike the other two valid classes, *C. perplexans*

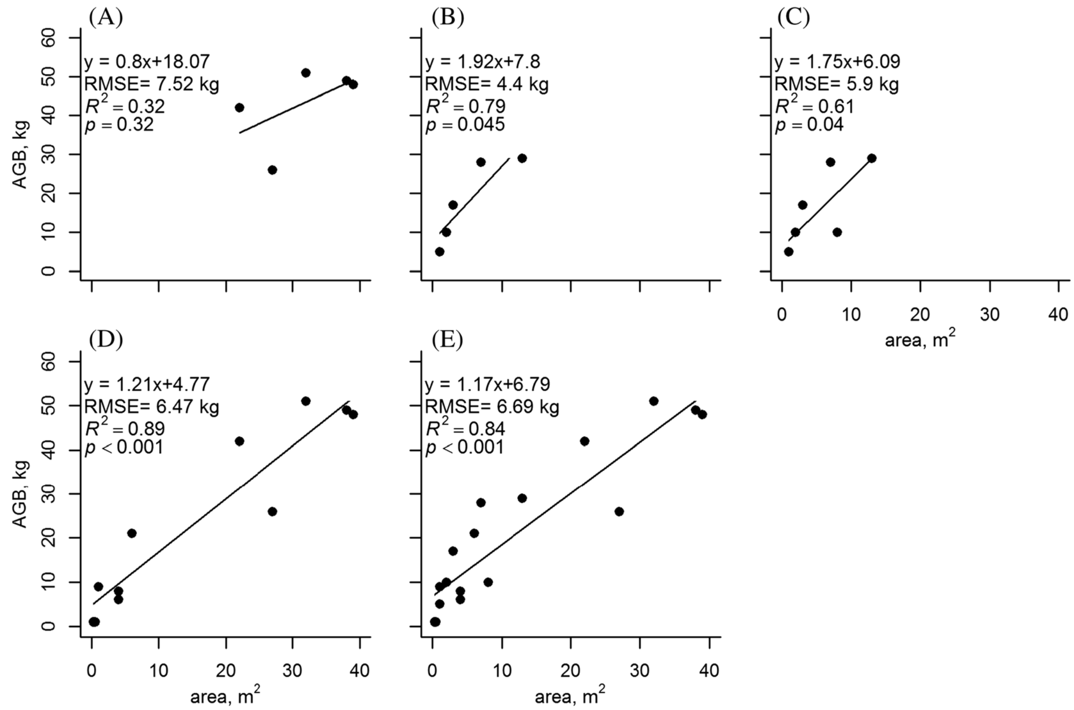

Fig. 4 Ordinary least square linear regression models at the Long Canyon study site. **a** *Adenostoma fasciculatum*, **b** *Ceanothus perplexans*, **c** group 1, **d** group 2, and **e** all-shrub

had comparable R^2 values between the Long Canyon and Kitchen Creek study sites, i.e., 0.79 vs. 0.84. Functional group 1 had a moderate R^2 value of 0.61, while *C. perplexans* alone had considerably higher value of 0.79. The shrub-pooled model yields an R^2 nearly as high as the group 2 model (0.84 vs. 0.89). This indicates that estimating generic shrub coverage, regardless of species-level class or pooled samples, may be suitable for estimating stand-level AGB in younger stands. This result differs between the two study areas; at the Kitchen Creek site, the groups and species-based models displayed the capability to yield higher accuracy AGB estimates. In addition, the slope values of the OLS models at the Long Canyon site are considerably lower than the Kitchen Creek site; this is very likely due to younger stand age occurring at the Long Canyon site. When upscaling AGB estimates in stands 7 years and younger, functional grouping may not yield reliable results as pooling samples for all shrubs.

Table 4 Cross-validation R^2 values

Classification	KC	LC
Quercus berberidifolia	0.87	Invalid
Adenostoma fasciculatum	0.94	Invalid
Ceanothus perplexans	0.17	Invalid
Arctostaphylos glandulosa	0.57	Invalid
All other shrubs	0.10	Invalid
Completely dead	Invalid	Invalid
Group 1	0.90	0.35
Group 2	0.96	0.80

The values under the KC heading are the results from the sampling plots at Kitchen Creek and LC are those in Long Canyon. Invalid results indicate a higher level of variability in the data set and therefore not being able to withstand the K-fold ($n-1$) process

Three of the six species-based classes at the Kitchen Creek site, *Q. berberidifolia*, *A. fasciculatum*, and *A. glandulosa*, yield suitable R^2 values when K-fold ($n-1$) is applied. All of the pooled groups have acceptable K-fold ($n-1$) R^2 at the Kitchen Creek site, including a model containing all of the "live and dead" shrub categories. All of the five species-level classes at the Long Canyon site have invalid cross-validation results likely due to small sample size ($n \leq 5$) and higher variability associated with a younger stand. The scatterplots containing the bivariate normal ellipses indicate that the K-fold ($n-1$) is fairly unbiased in terms of overestimating or underestimating fuel loads, although the ellipses in both study areas are slightly tilted upward

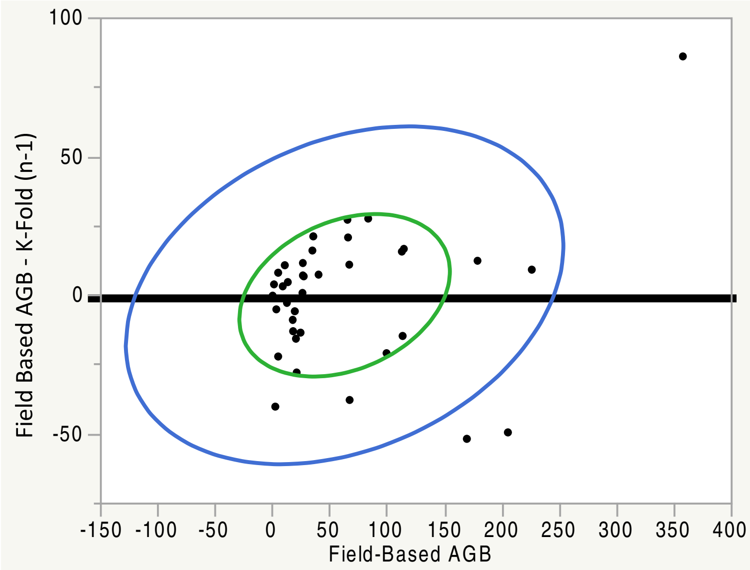

Fig. 5 Scatterplot of field-based AGB (kg) estimates (*x*-axis) against field-based estimates minus K-fold ($n-1$) predicted values (*y*-axis) at the Kitchen Creek study site. The *green ellipse* is a bivariate normal ellipse (p = .50). The *blue ellipse* is a bivariate normal ellipse (p = .95)

at the higher end of the AGB levels. This result indicates that the sampling plots with greater AGB were slightly underestimated, and the sampling plots with less AGB were slightly overestimated. The K-fold ($n-1$) scatterplots also show the levels of variability between the Kitchen Creek and Long Canyon study sites. The scatterplots show a much higher percentage of points that fall into the bivariate normal ellipse (p = .50) in the Kitchen Creek scatterplot relative to the Long Canyon scatterplot, and this indicates a higher level of variability.

In summary, the K-fold ($n-1$) indicated that the OLS models should allow stable and realistic AGB estimates when using the all-shrub pooled models and groups at both study areas. In the older stands found at Kitchen Creek, the OLS models can strongly predict fuel loads at the group level (and in two of the six species-level classes if so desired). These results support the potential of upscaling to stands or GRE derived from satellite imagery by showing stability in fuel load levels when data are pooled in the group and all-shrub groupings. Upscaling estimates increase the efficiency of estimating fuel loads by using mapped shrub coverage rather than directly linking ground coverage to field-based measurements.

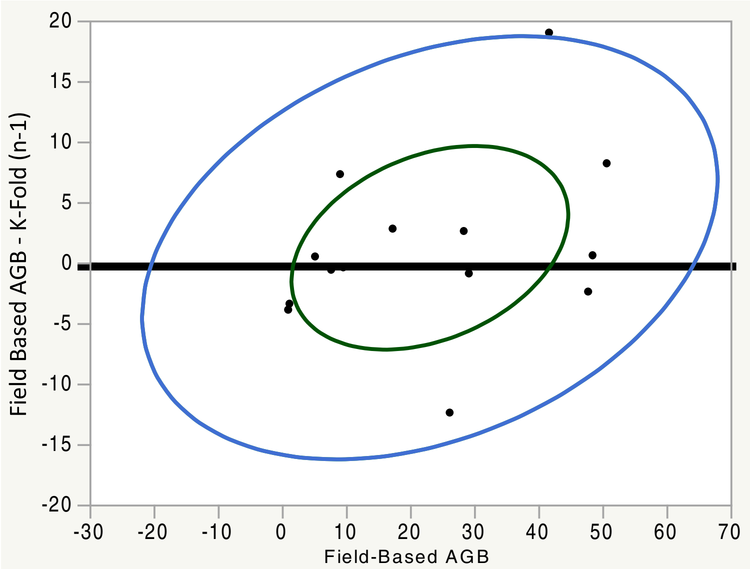

Fig. 6 Scatterplot of field-based AGB (kg) estimates (*x*-axis) against field-based estimates minus K-fold ($n-1$) predicted values (*y*-axis) at the Long Canyon study site. The *green ellipse* is a bivariate normal ellipse (p = .50). The *blue ellipse* is a bivariate normal ellipse (p = .95)

A. fasciculatum is known to have different burning properties than the other dominant shrub species found in chaparral (Sun et al. 2006). *A. fasciculatum* is the most flammable shrub, while the other shrubs burn longer once ignited. Through this study, we developed methods to identify *A. fasciculatum* in mixed chaparral and accurately estimated fuel loads in 28+-year-old stand ages by using ground coverage estimates as the predictor variable in linear regression models. The methods could also be used to estimate the relative fuel load and ground coverage of *A. fasciculatum* relative to other shrubs in mixed chaparral, e.g., to obtain percentage ground cover of *A. fasciculatum*. A study in the Sierra Nevada measuring *A. fasciculatum* growth rates in different stand ages showed the greatest amount of growth 2 to 16 years after burning and a maximum fuel load at 35 years since last fire (Rundel and Parsons 1979). Mooney (1981) reports comparable biomass accumulation figures in postburn *A. fasciculatum* with biomass amounts beginning to level off 20 to 25 years following fire. We found a similar relationship. The young stand had much less fuel than the older stands. The stands at the Kitchen Creek site (28 years and older) showed similar fuel load levels to the study in the Sierra Nevada, indicating that both may have reached the upper threshold of fuel accumulation (Rundel and Parsons 1979).

This study demonstrates that ultra-high spatial resolution (5 to 7 cm ground sampling distance) aerial RGB imagery enabled identification of the shrub species and estimating ground coverage within the study area when the image spatial resolution is extremely high. The majority of fuel load studies in the past have examined vegetation indices using color infrared (CIR) imagery. Although it has proven useful, CIR imagery is not as readily available, particularly at ultra-high spatial resolution (Lu 2006).

Estimating fuel loads using basal area measurements, regression equations, and image-based estimates of shrub ground coverage is demonstrated to be a suitable method in chaparral vegetation 7 years since last burned and older if species-based classes were pooled into functional and all-shrub groups. The K-fold $(n-1)$ indicates a high level of stability for biomass per area relationships when samples were pooled into groups for three of the six classes at the Kitchen Creek site. The slope values (beta coefficients) of the linear regression models of AGB vs. area of coverage in all classes and groups were three to five times greater in the older stands found at the Kitchen Creek site relative to the younger stand at the Long Canyon site. At the Kitchen Creek site, OLS models were suitable except for the completely dead class, which is likely due to difficulty in identification with a nadir perspective associated with remote sensing. In the young stand within the Long Canyon site, species-based models were not suitable, except for *C. perplexans.* The species-level linear models from the Kitchen Creek study area allowed for the identification of functional groups by comparing model parameters. Combining the data into the functional groups in addition to an all-shrub class yielded suitable linear models and cross-validation results in all of the burn history areas. The cross-validation and pooling results indicate the high potential for upscaling fuel load estimates to broader areal extents. The next research step (not included in this study) should involve mapping functional groups over larger extents and applying AGB/area measures to estimate total AGB over larger areas of vegetation.

Fuel models are often represented by a homogenous depiction of vegetation assemblages, and more spatially detailed models should increase the accuracy of wildfire behavior models when such models are capable of incorporating greater detail (Rollins et al. 2004). Shrublands occurring in Mediterranean-type climate areas are prone to devastating wildfires that threaten human life and have the capability to destroy thousands of structures (Rundel 1998). This is especially critical considering the increase in human population and the associated growth of urban areas into these fire-prone shrublands (Syphard et al. 2012). Further, accurate estimation and assessment of shrubland wildfire fuel loads are vitally important, especially in light of the influence of climate change on future fire regimes in Mediterranean-type climate shrublands (Keeley and Fothringham 2002). When considering fire suppression efforts, the only factor that humans can manipulate is the wildfire fuels (Rothermel 1972). This study shows that estimating the spatial distribution of shrubland fuel loads using remote sensing methods in tandem with field-based measurements should be achievable at the species level in older stands (e.g., mixed chaparral) and on functional groups in younger stands. While chaparral shrublands were the focus of this study, our results are potentially applicable to other shrublands (Rundel and Parsons 1979).

Acknowledgments We thank J. Truett, T. Hayes, and J. Kraling from the USFS for arranging site access. We also thank D. Rachels, C. Riggan, A. Brown, F. Uyeda, J. Jesu, B. Lo, B. Corcoran, D. Smith, and Y. Granovskaya for their assistance in the field, and we thank two anonymous reviewers whose suggestions greatly improved the manuscript. Richard McCreight of NEOS, LTD.

provided ultra-high spatial resolution aerial imagery. Funding for this project was provided by the USFS Recovery Act Agreement No. 10-JV-11279701-10: Airborne remote sensing to enable hazardous fuels reduction, forest health protection, rehabilitation, and hazard mitigation activities on federal lands.

References

Arroyo, L., Pascual, C., & Manzanera, J. (2008). Fire models and methods to map fuel types: the role of remote sensing. *Forest Ecology and the Environment, 256*, 1239–1252.

Baskerville, G. (1972). Use of logarithmic regression in the estimation of plant biomass. *Canadian Journal of Forest Research, 2*, 49–53.

Bowman, R. (1973). Soil survey of the San Diego area, California. Part I. United States Department of Agriculture, Soil Conservation Service and Forest Service, Washington, D.C., USA.

Catchpole, W., & Wheeler, C. (1992). Estimating plant biomass: a review of techniques. *Australian Journal of Ecology, 17*, 121–131.

Chen, W., Blain, D., Li, J., Keohler, K., Fraser, R., Zhang, Y., Leblanc, S., Olthof, I., Wang, J., & McGovern, M. (2009). Biomass measurements and relationships with Landsat-7/ETM+ and JERS-1/SAR data over Canada's western sub-arctic and low arctic. *International Journal of Remote Sensing, 30*, 2355–2376.

Conard, S. & Weise, D.R. (1998). Management of fire regime, fuels, and fire effects in southern California chaparral: lessons from the past and thoughts for the future. Tall Timbers Fire Ecology Conference Proceedings, 20, 342–350.

Countryman, C. (1972). The fire environment concept. U.S. Dept. of Agriculture Forest Service. Pacific Southwest Forest and Range Experiment Station, Berkeley, CA, 12p.

Dennison, P., Roberts, D., & Reggelbrugge, J. (2006). Characterizing chaparral fuels using combined hyperspectral and synthetic aperture radar data. *International Journal of Remote Sensing, 26*, 1035–1042.

Eisfelder, C., Kuenzer, C., & Dech, S. (2011). Derivation of biomass information for semi-arid areas using remote-sensing data. *International Journal of Remote Sensing, 33*(9), 2937–2984.

Garcia, M., Riano, D., Chivieco, E., & Danson, F. (2010). Estimating biomass carbon stocks for a Mediterranean forest in central Spain using LiDAR height and intensity data. *Remote Sensing of Environment, 114*, 816–830.

Hanes, T. (1971). Succession after fire in the chaparral of Southern California. *Ecological Monographs, 40*(1), 27–52.

Horton, J., & Kraebel, C. (1955). Development of vegetation after fire in the chamise chaparral of Southern California. *Ecology, 36*, 244–262.

Jensen, J.R. (2005). Introductory digital image processing, a remote sensing perspective. Prentice Hall Series in Geographic Information Science. Pearson Education. 3rd edition.

Keeley, J. E. (1991). Seed germination and life history syndromes in the California chaparral. *Botanical Review, 57*, 81–116.

Keeley, J. E., & Fothringham, C. J. (2002). Impact of past, present, and future fire regimes on North American Mediterranean shrublands. In T. T. Veblen, W. L. Baker, G. Montenegro, & T. W. Swetman (Eds.), *Fire and climate change in temperate ecosystems of the western Americas* (pp. 218–262). New York: Springer.

Kohavi, R. (1995). A study of cross validation and bootstrap accuracy validation and model selection. In *International Joint Conference on Artificial Intelligence. IJCAI'95 Proceedings of the 14th International Joint Conference* (Vol. 2). San Francisco: Morgan Kaufman Publishers, Inc..

Lu, D. (2006). The potential and challenge of remote sensing-based biomass estimation. *International Journal of Remote Sensing, 27*(7), 1297–1328.

Mooney, H. A. (1981). Primary production in Mediterranean-climate regions. In F. DiCastri & D. W. Goodall (Eds.), *Ecosystems of the world: Mediterranean-type shrublands* (pp. 249–255). New York: Elsevier Scientific.

Nijland, W., Addink, E., De Jong, S., & Van Der Meer, F. (2009). Optimizing spatial image support for quantitative mapping of natural vegetation. *Remote Sensing of the Environment, 113*, 771–780.

PRISM Climate Group (2014). Oregon State University, http://www.prism.oregonstate.edu/documents/PRISM_terms_of_use.pdf. Accessed 4 April 2014

Riggan, P. J., Goode, S., Jacks, P. M., & Lockwood, R. N. (1988). Interaction of fire and community development in chaparral of Southern California. *Ecological Monographs, 58*(3), 155–176.

Riggan, P. J., Franklin, S., Brass, J., & Brooks, F. (1994). Perspectives on fire management in Mediterranean ecosystems of southern California. In J. M. Moreno & W. C. Oechel (Eds.), *The role of fire in Mediterranean-type ecosystems* (pp. 140–162). New York: Springer.

Rollins, M., Keane, R., & Parsons, R. (2004). Mapping fuels and fire regimes using remote sensing, ecosystem simulation, and gradient modeling. *Ecological Applications, 14*(1), 75–94.

Rothermel, R. (1972). A mathematical model for predicting fire spread in wildland fuels. USDA Forest Service. Research Paper INT-115.

Rundel, P. W. (1998). Landscape disturbance in Mediterranean-type ecosystems: an overview. In P. W. Rundel, G. Montenegro, & F. M. Jaksic (Eds.), *Landscape disturbance and biodiversity in Mediterranean-type ecosystems* (pp. 3–22). New York: Springer.

Rundel, P. W., & Parsons, D. J. (1979). Structural changes in chamise (*Adenostoma fasciculatum*) along a fire-induced age gradient. *Journal of Range Management, 32*, 462–466.

Sprugel, D. (1983). Correcting for bias in log-transformed allometric equations. *Ecology, 64*, 209–210.

Sun, L., Zhou, X., Mahalingham, S., & Weise, D. (2006). Comparison of burning characteristics of live and dead chaparral fuels. *Combustion and Flame, 144*(1–2), 349–359.

Syphard, A. D., Keeley, J. E., Massada, A. B., Brennan, T. S., & Radeloff, V. C. (2012). Housing arrangement and location determine the likelihood of housing loss due to wildfire. *PloS One, 7*(3), 1–13.

Uyeda, K. A., Stow, D. A., O'Leary, J. F., Schmidt, I. T., & Riggan, P. J. (2016). Spatial variation of fuel loading within varying aged stands of chaparral. *Applied Vegetation Science, 19*(2), 267-279